Fuzzy and 2-DOF Controllers for Processes with a Discontinuously Variable Parameter

Alexandra-Iulia Szedlak-Stinean[1], Radu-Emil Precup[1] and Emil M. Petriu[2]
[1]*Department of Automation and Applied Informatics, Politehnica University of Timisoara, Bd. V. Parvan 2, 300223, Timisoara, Romania*
[2]*School of Electrical Engineering and Computer Science, University of Ottawa, 800 King Edward, K1N 6N5, Ottawa, ON, Canada*

Keywords: Classical PID Controllers, Digital and Experimental Results, Flexible Drive Dynamics, Fuzzy Controllers, Mechatronics Application, Two-Degree-of-Freedom PID Controllers, Variable Moment of Inertia.

Abstract: The application with a discontinuously variable parameter (moment of inertia) discussed in this paper is represented by an experimental setup, namely the Model 220 Industrial Plant Emulator (M220IPE), which allows the testing of several control solutions by performing real-time experiments. This paper suggests a simple state feedback control structure with three position controllers developed with the aid of linearized mathematical models and particular features of the process. The control structures contain conventional controllers (PID) and also advanced control solutions (Takagi-Sugeno PD+I fuzzy and two-degree-of-freedom PID controllers). The aim of these control structures is to achieve good robustness, good disturbance control behaviours regarding the model uncertainties and also to improve set-point responses. The proposed control structures are validated by digital and experimental results obtained for three specific values of the moment of inertia.

1 INTRODUCTION

Over the past two decades, the development of mechatronics systems has led to a novel stage of engineering design. By constantly evolving, these systems exhibit increasing performances ensuring, as shown in (Isermann, 2005), applicative and functional versatility, intelligence and flexibility. Since in various fields very good performance specifications are imposed, the design of the control systems is also important. If several process operating conditions (e.g., moment of inertia) are involved as variable parameters, the imposed specifications become even more restrictive. In this regard, the degree of complexity of the control subsystem of a mechatronics application differs from one application to another and may include relatively simple and advanced control structures as well.

The representative mechatronics system described in this paper considers a nonlinear and complex laboratory equipment with adjustable inertia (ECP, 2010). One of the purposes of this paper is to illustrate how the use of laboratory equipment of medium complexity and of different control structures can be made accessible, easily understandable and increasingly attractive.

In this paper design and implementation details are given regarding a state feedback control structure (SFCS) for M220IPE with flexible drive dynamics. The use of an SFCS offers no guarantee for the zero steady-state control error. Taking into account that the transfer function (t.f.) related to the inner control loop has two real poles and two complex conjugated poles, including the integral term in the state feedback control in terms of extending the state does not assure the imposed performance requirements (reduced settling times and phase margins of 60°). That is the reason why the SFCS is inserted in a control loop that contains three types of position controllers: (1) a PID controller, (2) a Takagi-Sugeno PD+I fuzzy controller (TS-PD+I-FC) and (3) a two-degree-of-freedom PID controller (2-DOF PID).

This paper offers fivefold contributions: 1. the mathematical modeling of M220IPE with flexible drive dynamics and the interpretation of these models as benchmark type MMs, 2. the design and implementation of the SFCS, 3. the development and verification through simulations and experiments of

Szedlak-Stinean, A-I., Precup, R-E. and Petriu, E.
Fuzzy and 2-DOF Controllers for Processes with a Discontinuously Variable Parameter.
DOI: 10.5220/0006468504310438
In *Proceedings of the 14th International Conference on Informatics in Control, Automation and Robotics (ICINCO 2017) - Volume 2*, pages 431-438
ISBN: Not Available

the proposed SFCS with PID controllers for nine cases, 4. the digital simulation and experimental testing of the SFCS with PID controllers, TS-PD+I-FCs and 2-DOF PID controllers in three most favorable case studies (i.e., the case studies I.a, II.b and III.c) dedicated to the position control of M220IPE with flexible drive dynamics, and 5. comparative analyses to prove the validity of all control solutions. They are relevant in the field as they offer cost-effective control structures, characterized by a simple structure, design and implementation.

The paper is divided into the following sections: the dynamic equations described in the process MM in case of flexible drive dynamics and the system parameters values are given in Section 2. The structural properties of the process and the design and implementation of the SFCS are offered in Section 3. Three positioning control structures developed for M220IPE with flexible drive dynamics are presented in Section 4. The digital simulation and experimental results obtained are shown in Section 5. The conclusions are highlighted in Section 6.

2 ELECTROMECHANICAL PLANT – M220IPE

The controlled system is a mechatronics application that is composed of three individual subsystems, namely the electromechanical component, the real-time controller unit and the dedicated executive software. The main subsystem is the electromechanical plant, which comprises a drive motor that is coupled to a drive disk by means of a timing belt, a disturbance motor that is coupled via a 4:1 gear ratio to a load disk and a speed reduction assembly that connects the drive and load discs.

The moment of inertia of the two discs can be adjusted by adding or removing specific weights (ECP, 2010; Stinean et al., 2013a; Stinean et al., 2013b). The electromechanical plant can emulate a variety of dynamic configurations tested by employing a nonlinear MM that closely describes the actual behaviour of the system. The schematic structure of the controlled process is illustrated in Figure 1.

2.1 Mathematical Models

The MM of the electromechanical plant with flexible drive dynamics can be determined using the relations (1) - (3), where the terms are described in (ECP, 2010; Stinean et al., 2013a; Stinean et al., 2013b; Stinean et al., 2015; Acho et al., 2013).

The dynamic equations that describe the process in case of flexible drive dynamics are:

$$\begin{aligned} &J_{dr}^{*}\ddot{\theta}_1+(c_1+c_{12}gr^{-2})\dot{\theta}_1-c_{12}gr^{-1}\dot{\theta}_2+kgr^{-2}\theta_1-kgr^{-1}\theta_2=T_D,\\ &J_{ld}\ddot{\theta}_2-c_{12}gr^{-1}\dot{\theta}_1+(c_2+c_{12})\dot{\theta}_2-kgr^{-1}\theta_1+k\theta_2=0. \end{aligned} \tag{1}$$

with J_{dr}^{*}, J_{dr}, J_p, J_{ld}, gr and gr' expressed as

$$\begin{aligned} &J_{dr}^{*}=J_{dr}+J_p(gr')^{-2}+J_{ld}(gr)^{-2},\\ &J_p=J_{p\_dr}+J_{p\_ld}+J_{backlash},\\ &J_{dr}=J_{d\_dr}+J_{w\_dr},\ J_{ld}=J_{d\_ld}+J_{w\_ld},\\ &gr=6n_{p\_d}/n_{p\_l},\ gr'=n_{p\_d}/12. \end{aligned} \tag{2}$$

The state-space MM (SS-MM) of M220IPE with flexible dynamics with θ_1 as the process output is

$$\begin{aligned} &\begin{cases}\mathbf{x}=\mathbf{A}\,\mathbf{x}+\mathbf{B}\,\mathbf{T}\\ y=\mathbf{C}\,\mathbf{x}\end{cases},\\ &\mathbf{x}=[\theta_1\ \ \theta_1\ \ \theta_2\ \ \theta_2]^T,\ \mathbf{A}=[a_{ij}]_{i,j=1\ldots4},\\ &\mathbf{B}=[b_{i1}]_{i=1\ldots4},\ \mathbf{C}=[c_{1j}]_{j=1\ldots4}. \end{aligned} \tag{3}$$

with the matrix elements shown in (4)

$$\begin{aligned} &a_{11}=0, a_{12}=1, a_{13}=0, a_{14}=0,\\ &a_{21}=-kgr^{-2}/J_{dr}^{*}, a_{22}=-(c_1+c_{12}gr^{-2})/J_{dr}^{*},\\ &a_{23}=kgr^{-1}/J_{dr}^{*}, a_{24}=c_{12}gr^{-1}/J_{dr}^{*},\\ &a_{31}=0, a_{32}=0, a_{33}=0, a_{34}=1,\\ &a_{41}=kgr^{-1}/J_{ld}, a_{42}=c_{12}gr^{-1}/J_{ld},\\ &a_{43}=-k/J_{ld}, a_{44}=-(c_2+c_{12})/J_{ld},\\ &b_{11}=0, b_{21}=1/J_{dr}^{*}, b_{31}=0, b_{41}=0,\\ &c_{11}=1, c_{12}=0, c_{13}=0, c_{14}=0. \end{aligned} \tag{4}$$

The application of the Laplace transform to (1) considering that the initial conditions are zero, leads to the following t.f.:

$$\begin{aligned} &\theta_1(s)/T_D(s)=[J_{ld}s^2+(c_2+c_{12})s+k]/d(s),\\ &d(s)=d_4s^4+d_3s^3+d_2s^2+d_1s,\\ &d_4=J_{dr}^{*}J_{ld}, \mathrm{d}_3=J_{dr}^{*}(c_2+c_{12})+\\ &+J_{ld}[c_1+c_{12}/(gr^2)], d_2=J_{dr}^{*}k+\\ &+J_{ld}k/(gr^2)+c_1c_2+c_1c_{12}+c_{12}c_2/(gr^2),\\ &d_1=c_1k+c_2k/(gr^2). \end{aligned} \tag{5}$$

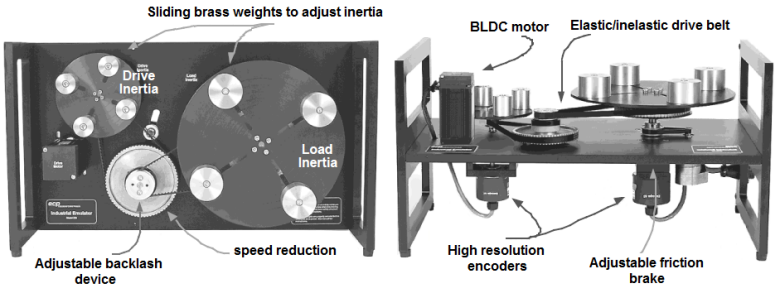

Figure 1: Electromechanical plant of M220IPE.

2.2 System Parameter Values

As given in the electromechanical plant manual (ECP, 2010) the parameter values used for the design of the SFCS are presented in Table 1.

Table 1: System parameter values.

Parameter values		
Parameters	Values	Remarks
J_{d_dr}	0.00040 [kgm^2]	
J_{d_ld}	0.0065 [kgm^2]	
$J_{backlash}$	0.000031 [kgm^2]	
J_{w_dr}	0.0021 [kgm^2]	4·0.2 kg at r_{w_dr}=0.05 m
J_{w_dr}	0.00561 [kgm^2]	4·0.5 kg at r_{w_dr}=0.05 m
J_{w_ld}	0.00824 [kgm^2]	4·0.2 kg at r_{w_ld}=0.1 m
J_{w_ld}	0.0206 [kgm^2]	4·0.5 kg at r_{w_ld}=0.1 m
J_{p_dr} or J_{p_ld}	0.000008 [kgm^2]	n_{p_d}=24 or n_{p_l}=24
J_{p_dr} or J_{p_ld}	0.000039 [kgm^2]	n_{p_d}=36 or n_{p_l}=36
c_1	0.004 [Nm/rad/s]	
c_2	0.05 [Nm/rad/s]	
c_{12}	0.017 [Nm/rad/s]	
k	8.45 [Nm/rad]	

Because the laboratory application does not allow a continuous moment of inertia variation, the proposed control solutions that will be implemented on M220IPE, analyzed and tested through digital simulations and experiments will be developed for three specific values of inertia of the load disk, J_{ld} (Stinean et al., 2013a; Stinean et al., 2013b; Stinean et al., 2015): the minimum value $J_{ld,min}$=0.0065 kgm^2 (load disk with no weights on it), the average value $J_{ld,avg}$=0.01474 kgm^2 (four 0.2 kg weights positioned at 0.1m from the load disk center) and the maximum value $J_{ld,max}$=0.0271 kgm^2 (four 0.5 kg weights positioned at 0.1m from the load disk center).

There are totally nine possible combinations between the process and controller parameters. The t.f. in (5) and the matrix coefficients for the three specific moment of inertia values are presented in Table 2.

3 STATE FEEDBACK CONTROL STRUCTURE

The use of the SFCS is based upon three main reasons: 1. the simultaneous control of all the essential process variables (state variables) and the design of the structure in relation to the evolution of these variables, 2. the stabilization of unstable processes, and 3. the possibility to achieve the zero static control error by extending the base structure.

The process structural properties are examined considering the linearized SS-MMs and accounting for the specific features of the nonlinearities. In this regard, the controllability test of the linearized SS-MMs (3) is conducted, using particularized parameter values corresponding to defined operating points. The state feedback controller contains a supplementary amplifier with the k_{AS} gain. Since the state feedback gain matrix $\mathbf{k_c}^T$ is of proportional type, the use of SFCS does not prove to be effective regarding the zero steady-state control error. The pole placement method is applied to develop our SFCS, namely to actually determine the parameter values of $\mathbf{k_c}^T$, using three sets of poles for each value of the moment of inertia of the load disk Using $e_x=w_x-y_x$, $y_x=\boldsymbol{k_c}^T\boldsymbol{x}$ and $u=k_{AS}e_x$, the SS-MM of the SFCS is

$$\begin{cases} \mathbf{x} = \mathbf{A}_x\,\mathbf{x} + \mathbf{B}\,k_{AS}w_x \\ y = \mathbf{C}\,\mathbf{x} \end{cases}, \tag{6}$$

where $\boldsymbol{A_x}=\boldsymbol{A}-\boldsymbol{B}\boldsymbol{k_c}^T k_{AS}$ is the system matrix of the inner loop, and k_{AS}=1. The expression of $\mathbf{k_c}^T$ is

$$\mathbf{k}_\mathbf{c}^\mathbf{T} = [k_{c1} \quad k_{c2} \quad k_{c3} \quad k_{c4}], \tag{7}$$

where T represents the transpose matrix and the gain values are given in Table 3, columns 5, 6, 7 and 8.
The poles for the closed-loop system are also given in Table 3 columns 1, 2, 3 and 4. The SS-MM of the inner control loop leads to the t.f.

$$H_{SFCS}(s) = \mathbf{C}(s\mathbf{I} - \mathbf{A}_x)^{-1}\mathbf{B} = \\ = \frac{k_{SFCS}(1 + 2\zeta_b T_b s + T_b^2 s^2)}{(1 + T_1 s)(1 + T_2 s)(1 + 2\zeta_a T_a s + T_a^2 s^2)}, \quad (8)$$

where T_1, T_2 are the large time constants, T_a is the equivalent time constant, and ζ_a is the damping coefficient.

4 POSITIONING CONTROL STRUCTURES FOR M220IPE WITH FLEXIBLE DRIVE DYNAMICS

This section presents the three proposed position control structures developed to achieve the zero steady-state control error specification, fulfilled by the integral component of the controllers.

4.1 PID Controllers

The first state feedback control solution uses a classical PID controller with the continuous-time t.f. and tuning equations

$$H_r(s) = k_r(1 + sT_{r1})(1 + sT_{r2})/s, \\ k_r = 1/(2k_{SFCS}T_2), T_{r1} = T_1, T_{r2} = T_2, \quad (9)$$

with k_r – the controller gain, and T_{r1} and T_{r2} – the controller time constants. After discretizing the continuous-time PID controller using the backwards difference method and setting the value of the sampling period to h=0.004 s, the discretized t.f. is

$$H_r(z^{-1}) = (q_0 + q_1 z^{-1} + q_2 z^{-2})/(p_0 + p_1 z^{-1}), \\ q_0 = K_p h + K_i h^2 + K_d, \\ q_1 = -(K_p h + 2K_d), \\ q_2 = K_d, p_0 = h, p_1 = -h, \quad (10)$$

where $K_p=k_r(T_{r1}+T_{r2})$, $K_i=k_r$ and $K_d=k_r T_{r1} T_{r2}$. The PID controller parameter values for three significant operating points obtained by Kessler's Modulus Optimum method (Åström and Hägglund, 1995) are shown in Table 4, column 3.

4.2 Takagi-Sugeno PD+I Fuzzy Controllers

Fuzzy controllers can be considered as easily understandable initial controllers (Guerra et al., 2015; Precup et al., 2015). This paper considers their design and tuning such as to merge separately designed linear controllers using the linearized process MM at several operating points, justified as our controllers behave like bumpless interpolators between linear controllers, which is important due to the nonlinear input-output map of fuzzy controllers and their adaptation to process parameter changes.

The Takagi-Sugeno PD+I fuzzy block contains the PD fuzzy controller in the parallel structure with an integral (I) controller, i.e., the integral component is implemented separately such that $u_k=u_{PDk}+u_{Ik}$, knowing that u_{Ik} represents the output of this I component. The PD quasi-continuous digital controller and its parameters are derived from the PD

Table 2: State-space MM matrices and transfer functions expressions for M220IPE with flexible drive dynamics.

Moment of inertia	Matrices **A**, **B** and **C**	Process transfer function $\theta_1(s)/T_D(s)$
$J_{ld,min}$	$\mathbf{A} = \begin{bmatrix} 0 & 1 & 0 & 0 \\ -1259 & -12.068 & 5036 & 10.13 \\ 0 & 0 & 0 & 1 \\ 325 & 0.654 & -1300 & -10.307 \end{bmatrix}, \mathbf{B} = \begin{bmatrix} 0 \\ 13850 \\ 0 \\ 0 \end{bmatrix}, \mathbf{C} = [1 \quad 0 \quad 0 \quad 0]$	$\frac{13850(s^2 + 10.307s + 1300)}{s(s^3 + 22.37s^2 + 2677.2s + 22078)}$
$J_{ld,avg}$	$\mathbf{A} = \begin{bmatrix} 0 & 1 & 0 & 0 \\ -1259 & -12.068 & 5036 & 10.13 \\ 0 & 0 & 0 & 1 \\ 145 & 0.3 & -579 & -4.59 \end{bmatrix}, \mathbf{B} = \begin{bmatrix} 0 \\ 13850 \\ 0 \\ 0 \end{bmatrix}, \mathbf{C} = [1 \quad 0 \quad 0 \quad 0]$	$\frac{13850(s^2 + 4.59s + 579)}{s(s^3 + 16.65s^2 + 1893.7s + 9827.4)}$
$J_{ld,max}$	$\mathbf{A} = \begin{bmatrix} 0 & 1 & 0 & 0 \\ -1259 & -12.068 & 5036 & 10.13 \\ 0 & 0 & 0 & 1 \\ 77.9 & 0.157 & -312 & -2.47 \end{bmatrix}, \mathbf{B} = \begin{bmatrix} 0 \\ 13850 \\ 0 \\ 0 \end{bmatrix}, \mathbf{C} = [1 \quad 0 \quad 0 \quad 0]$	$\frac{13850(s^2 + 2.47s + 312)}{s(s^3 + 14.53s^2 + 1599.4s + 5290.4)}$

Table 3: Numerical values of the selected poles and state feedback gain matrix.

Moment of inertia	Flexible drive dynamics							
	Selected poles				State feedback gain matrix			
0	*1*	*2*	*3*	*4*	*5*	*6*	*7*	*8*
	p_1^*	p_2^*	p_3^*	p_4^*	k_{c1}	k_{c2}	k_{c3}	k_{c4}
$J_{ld,min}$	-12.26	-48.49	-28.32+59.3317i	-28.32-59.3317i	0.3234	0.0069	-0.7223	0.0247
$J_{ld,avg}$	-8.33	-26.32	-17.52+38.4817i	-17.52-38.4817i	0.0749	0.0038	-0.1030	0.0124
$J_{ld,max}$	-4.95	-16.46	-17.38+31.3767i	-17.38-31.3767i	0.0280	0.0030	-0.0155	0.0104

component by using

$$u_{PDk} = k_1\Delta e_k + k_2 e_k = k_1(\Delta e_k + \alpha e_k),$$
$$k_1 = K_d/h, k_2 = K_p, \alpha = k_2/k_1 = K_p h/K_d, \quad (11)$$

where $\Delta e_k = e_k - e_{k-1}$ represents the increment of the control error, e_k is the control error and u_{PDk} represents the output of the PD fuzzy controller. The developed TS-PD+I-FC substitutes the linear PD component in the linear PID controller presented in Sub-section 4.1. The fuzzification in TS-PD-FC is realized using for each input, three input linguistic terms LT_{ek} and $LT_{\Delta ek} \in$ {N, ZE, P} with trapezoidal and triangular membership functions μ_e, $\mu_{\Delta e}$. The involved operators from the inference engine are SUM and PROD and for defuzzification the weighted average method is employed. In total for the complete rule base, there are nine rules:

$$\begin{aligned}
&\text{If}(e_k \text{ is N and } \Delta e_k \text{ is P}) \text{ then } u_{PDk} = u_{PDk}^{\ a},\\
&\text{If}(e_k \text{ is ZE and } \Delta e_k \text{ is P}) \text{ then } u_{PDk} = u_{PDk}^{\ b},\\
&\text{If}(e_k \text{ is P and } \Delta e_k \text{ is P}) \text{ then } u_{PDk} = u_{PDk}^{\ c},\\
&\text{If}(e_k \text{ is N and } \Delta e_k \text{ is ZE}) \text{ then } u_{PDk} = u_{PDk}^{\ b},\\
&\text{If}(e_k \text{ is ZE and } \Delta e_k \text{ is ZE}) \text{ then } u_{PDk} = u_{PDk}^{\ c},\\
&\text{If}(e_k \text{ is P and } \Delta e_k \text{ is ZE}) \text{ then } u_{PDk} = u_{PDk}^{\ a},\\
&\text{If}(e_k \text{ is N and } \Delta e_k \text{ is N}) \text{ then } u_{PDk} = u_{PDk}^{\ c},\\
&\text{If}(e_k \text{ is ZE and } \Delta e_k \text{ is N}) \text{ then } u_{PDk} = u_{PDk}^{\ a},\\
&\text{If}(e_k \text{ is P and } \Delta e_k \text{ is N}) \text{ then } u_{PDk} = u_{PDk}^{\ b},
\end{aligned} \quad (12)$$

where $\chi \in \{a,b,c\}$ indicates the indices of the linear PD controllers, namely *a* for *C*-$J_{ld,min}$, *b* for *C*-$J_{ld,avg}$, and *c* for *C*-$J_{ld,max}$:

$$u_{PDk}^{\ \chi} = [K_d^{\ \chi}(\Delta e_k + \alpha^{\chi} e_k)]/h. \quad (13)$$

The parameter $B_{\Delta e}$ is obtained by the modal equivalence principle using the tuning equation $B_{\Delta e} = \min(\alpha^{\chi})B_e$, in which the B_e parameter is specified by the designer. The numerical values related to TS-PD+I-FCs for three specific values of the load disk moment of inertia are summarized in Table 4, column 4.

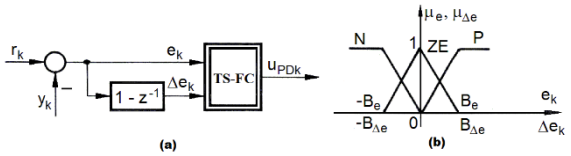

Figure 2: TS-PD-FC structure (a) and input membership functions (b).

4.3 2-DOF PID Controllers

The advantages of using 2-DOF control solutions are well known and concern reference tracking, disturbance rejection and simultaneous good feedback properties. Since multi-objective problems must be solved to design control systems, a 2-DOF controller has several advantages over a 1-DOF controller, shown in (Leva and Bascetta, 2006). The 2-DOF control structure illustrated in Figure 3 in a formulation based on PID controllers is referred to as 2-DOF PID controller structure. Over the past two decades many 2-DOF PID structures have been developed (Leva and Bascetta, 2006; Alfaro et al., 2009; Kevickzy and Banyasz, 2015), but in this paper this structure was chosen for two main reasons: 1. the simplicity of the structure, and 2. the ease of transforming the PID controller into a 2-DOF controller and vice versa. Using (Precup and Preitl, 2007; Precup et al., 2014), the main PID controller component $C^*(s)$ and the additional block $C_{FB}(s)$, highlighted in Figure 3, are described by the t.f.s

$$\begin{aligned}
&C^*(s) = k_C[(1-\tau) + \frac{1}{sT_i} + (1-\mu)D(s)],\\
&C_{FB}(s) = k_C[\tau + \mu D(s)]\\
&D(s) = \frac{sT_d}{1+sT_f},
\end{aligned} \quad (14)$$

where k_C, T_i, T_d, T_f are the tuning parameters for the 2-DOF PID controller, $k_C(1-\tau)=K_p$, $T_i=k_C/K_i$ and $T_d(1-\mu)=K_d$.

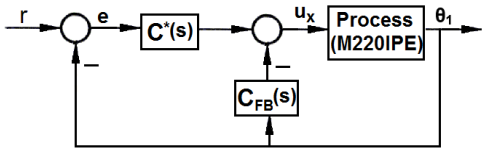

Figure 3: 2-DOF PID structure.

The parameter values employed in the design of this control solution are presented in Table 4, column 5.

5 DIGITAL AND EXPERIMENTAL RESULTS

The SFCS described in Section 3 was developed and tested on the M220IPE laboratory equipment in the framework of three proposed position control solutions. The parameter referred to as hardware gain k_{hw}=5.81 Nm/rad has been inserted in order to achieve a higher controller internal numerical resolution. This parameter also improves the encoder pulse period measurement (ECP, 2010).

In order to avoid the oscillations produced by the pair of complex conjugated poles and by the process nonlinearities, four real poles were considered for the proposed state feedback control solution. Because the results are approximately similar with the ones presented in this paper, this situation will not be discussed any further, but the idea how the poles of the inner loop can be modified may be the subject of future research.

Analyzing the comparative simulation and experimental results presented in Figure 4, the following aspects can be concluded: in terms of the best quality indices, both simulation and experimental results show that the best performances have been achieved in the cases I.a, II.b and III.c. The case I.a is more effective – concerning the settling time value (t_s≈0.8661s) and also overshoot value (σ_1≈0%) – than the cases I.b and I.c; regarding the overshoot values, the cases I.b and I.c exceed 22%; the case I.a offers the highest performance in both digital and experimental results and the worse result is obtained by the case I.c; the case II.b exhibits the highest performance regarding the settling time value (t_s≈1.1031) compared to the cases II.a (t_s≈1.6604s) and II.c (t_s≈2.3932s); the overshoot value in this case is around 8.65%; the case III.c has reached the highest performance indices concerning the settling time value (t_s≈1.8006s) and first settling time value (t_1≈0.2836s) compared to the cases III.a (t_s≈2.9723, t_1≈2.9521s) and III.b (t_s≈2.0981s, t_1≈2.0853); the case III.a was the slowest one by exhibiting the largest settling time value.

The three proposed position control solutions described in Section 4 were tested and validated for the electromechanical plant with flexible dynamics only in the three most favourable cases – case I.a, case II.b and case III.c – and the results are presented in Figure 5. Taking this into account, by comparing the achieved results, following conclusions can be drawn: (1) the PID control solution was used for comparison and also for the design of the other solutions; it was the least favourable one achieving poor results in both settling time and first settling time; (2) the 2-DOF PID control solution is more effective – in all three cases concerning the settling time and the first settling time – in comparison with the PID control solution, but worst in comparison to the TS-PD+I-FC control solution; (3) all proposed solutions showed good reference tracking behaviour and (4) the suggested position controllers contribute in average to both robustness and good dynamic performance regarding at least one process parameter. Other effects will be pointed out for other relevant applications including those presented in (Filip, 2008; Mazdin et al., 2016).

6 CONCLUSIONS

This paper provided details regarding the development of SFCSs aimed to control the position for a mechatronics system built round the M220IPE laboratory equipment. Since an SFCS doesn't guarantee the zero steady-state control error, therefore it is included in a control loop that contains three possible control structures with PID, TS-PD+I-FC and 2-DOF PID controllers. Digital and experimental results are given for three specific load disk moment of inertia values.

The step responses in relation to the reference input are used in the control structures comparison. The comparison shows that the suggested solutions are transparent and relatively easy to understand and to employ, and the best reference tracking and control system performance has been obtained in the cases I.a, II.b and III.c. The controller C-$J_{ld,\min}$ is suitable for $J_{ld,min}$ and less suitable for $J_{ld,avg}$ and $J_{ld,max}$. The controller C-$J_{ld,avg}$ is suitable for $J_{ld,avg}$ and less suitable for $J_{ld,min}$ and $J_{ld,max}$. The controller C-$J_{ld,max}$ is suitable for $J_{ld,max}$ and less suitable for $J_{ld,\min}$ and $J_{ld,avg}$.

The performance indices improvement for the proposed control solutions using both model-based and model-free tuning techniques will be the target of future research. In addition, the pole placement will be replaced with optimal parameter tuning.

ACKNOWLEDGEMENTS

This work was supported by grants from the Romanian Executive Agency for Higher Education, Research, Development and Innovation Funding (UEFISCDI), project number PN-II-RU-TE-2014-4-0207, the Partnerships in priority areas – PN II program of UEFISCDI, project numbers PN-II-PT-PCCA-2013-4-0544 and PN-II-PT-PCCA-2013-4-0070, and the NSERC of Canada.

Table 4: SFCS t.f.s. and numerical values of PID, TS-PD+I-FC and 2-DOF PID controllers.

Moment of inertia	Flexible drive dynamics									
	SFC structure t.f. $H_{SFCS}(s)$	*PID*			*TS-PD+I-FC*			*2-DOF PID*		
		3			4			5		
1	2	K_p	K_i	K_d	k_1	k_2	α	k_C	T_i	T_d
$J_{ld,min}$	$\frac{6.9503(1+0.0079s+0.00077s^2)}{(1+0.0206s)(1+0.0815s)(1+0.0131s+0.000231s^2)}$	0.1123	1.1	0.0018	0.4617	0.1123	0.2433	0.1127	0.1024	0.0074
$J_{ld,avg}$	$\frac{20.4588(1+0.0079s+0.00172s^2)}{(1+0.0379s)(1+0.12s)(1+0.0196s+0.000559s^2)}$	0.1105	0.7	0.0032	0.7981	0.1105	0.1384	0.1108	0.1584	0.0142
$J_{ld,max}$	$\frac{41.2229(1+0.0079s+0.0032s^2)}{(1+0.0607s)(1+0.202s)(1+0.0270s+0.000777s^2)}$	0.0919	0.35	0.0043	1.0729	0.0919	0.0857	0.0925	0.2643	0.0287

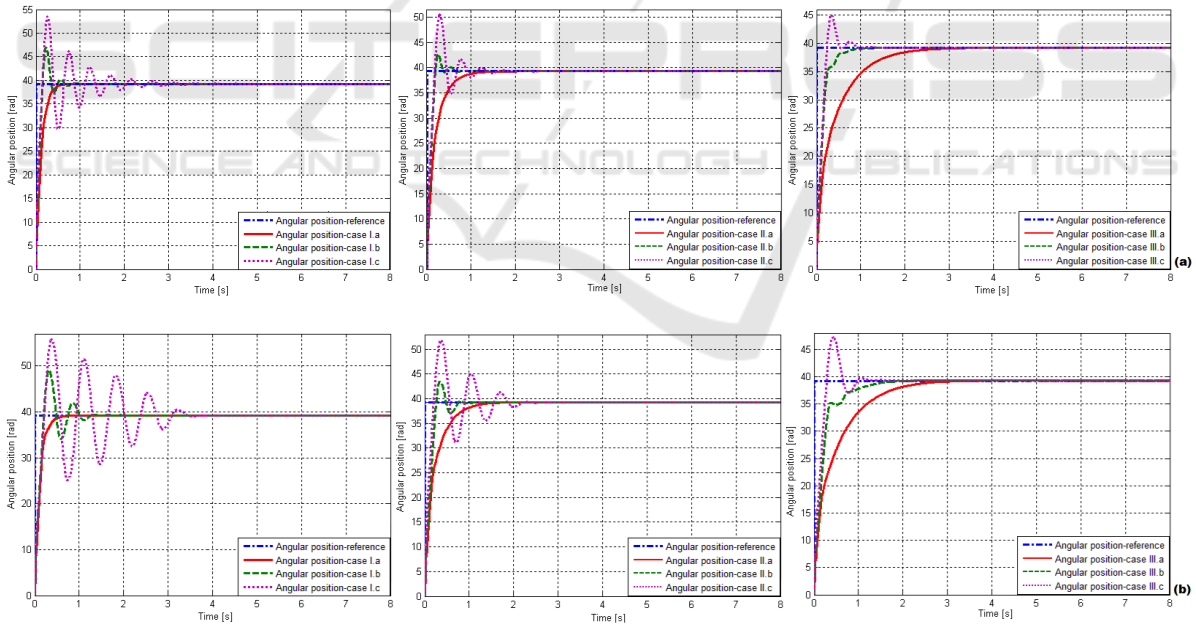

Figure 4: Digital (a) and experimental (b) results concerning the behaviour of SFCs with PID controllers designed for M220IPE with flexible drive dynamics: cases I.a-I.c, cases II.a-II.c and cases III.a-III.c.

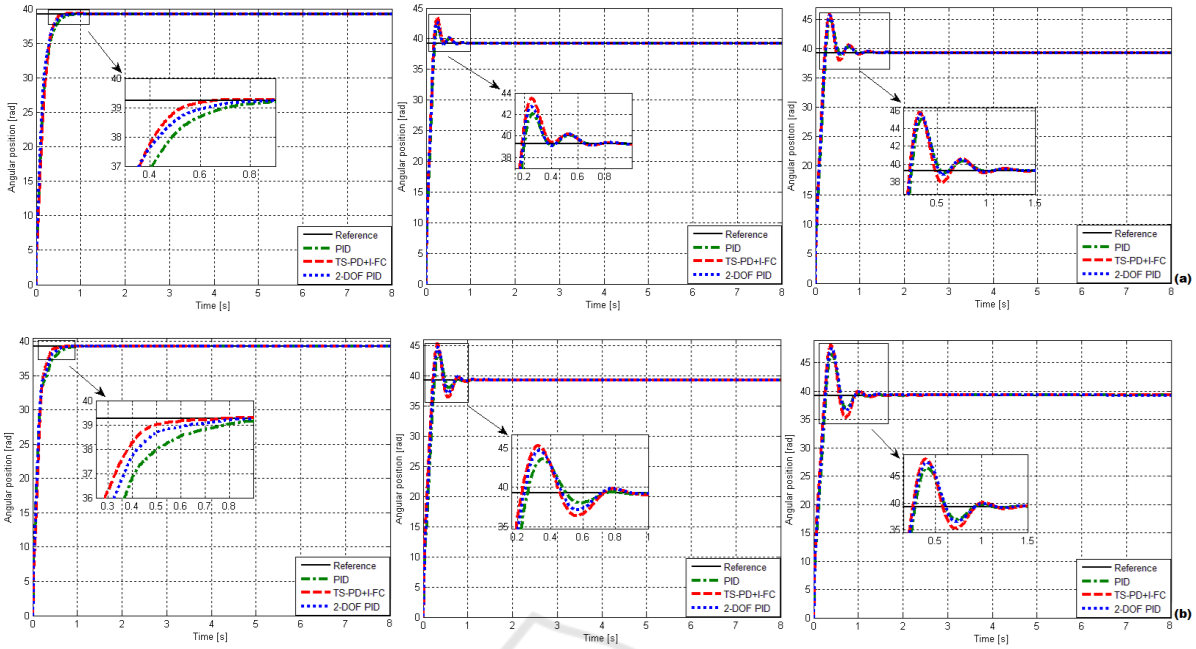

Figure 5: Digital (a) and experimental (b) results concerning the behaviour of SFCS with three proposed control solutions developed for M220IPE with flexible drive dynamics: case I.a, case II.b and case III.c.

REFERENCES

Acho, L., Ikhouane, F., Pujo, G., 2013. Robust control design for mechanisms with backlash. *Journal of Control Engineering and Technology*. 3, 175–180.

Alfaro, V. M., Vilanova, R., Arrieta, O., 2009. Robust tuning of Two-Degree-of-Freedom (2-DoF) PI/PID based cascade control system. *Journal of Process Control*. 19, 1658–1670.

Åström, K. J., Hägglund, T., 1995. *PID Controllers Theory: Design and Tuning*. Research Triangle Park, NC: Instrument Society of America.

ECP. 2010. *Industrial Emulator/Servo Trainer Model 220 System, Testbed for Practical Control Training*. Bell Canyon, CA: Educational Control Products.

Filip, F. G., 2008. Decision support and control for large-scale complex systems. *Annual Reviews in Control*. 32, 61–70, Apr. 2008.

Guerra, T. M., Sala, A., Tanaka, K., 2015. Fuzzy control turns 50: 10 years later. *Fuzzy Sets and Systems*. 281, 168–182.

Kevickzy, L., Banyasz, C., 2015. *Two-Degree-of-Freedom Control Systems: The Youla Parameterization Approach*. Academic Press, Elsevier.

Leva, A., Bascetta, L., 2006. On the design of the feed-forward compensator in two-degree-of-freedom controllers. *Mechatronics*, 16, 533–546.

Isermann, R., 2005. *Mechatronic Systems: Fundamentals*. Berlin, Heidelberg, New York: Springer-Verlag.

Mazdin, P., Arbanas, B., Haus, T., Bogdan, S., Petrovic, T., Miskovic, N., 2016. Trust consensus protocol for heterogeneous underwater robotic systems. *IFAC-PapersOnLine*, 49, 341–346.

Precup, R.-E., Angelov, P., Costa, B. S. J., Sayed-Mouchaweh, M., 2015. An overview on fault diagnosis and nature-inspired optimal control of industrial process applications, *Computers in Industry*. 74, 75–94.

Precup, R.-E., David, R.-C., Petriu, E. M., Preitl, S., Radac, M.-B., 2014. Novel adaptive charged system search algorithm for optimal tuning of fuzzy controllers. *Expert Systems with Applications*. 41, 1168–1175.

Precup, R.-E., Preitl, S., 2007. PI-fuzzy controllers for integral plants to ensure robust stability. *Information Sciences*. 177, 4410–4429.

Stinean, A.-I., Bojan-Dragos, C.-A., Precup, R.-E., Preitl, S., Petriu, E. M., 2015. Takagi-Sugeno PD+I fuzzy control of processes with variable moment of inertia. In *Proc. 2015 International Symposium on Innovations in Intelligent Systems and Applications*. Madrid, Spain, 1-8.

Stinean, A.-I., Preitl, S., Precup, R.-E., Dragos, C.-A., Radac, M.-B., Petriu, E. M., 2013a. Modeling and control of an electric drive system with continuously variable reference, moment of inertia and load disturbance. In *Proc. 9th Asian Control Conference*. Istanbul, Turkey, 1–6.

Stinean, A.-I., Preitl, S., Precup, R.-E., Dragos, C.-A., Radac, M.-B., Petriu, E. M., 2013b. Low-cost neuro-fuzzy control solution for servo systems with variable parameters. In *Proc. 2013 IEEE International Conference on Computational Intelligence and Virtual Environments for Measurement Systems and Applications*. Milano, Italy, 156–161.